Important Notice to Authors

No further publication processing will occur until we receive your response to this proof.

Attached is a PDF proof of your forthcoming article in PRB. Your article has 9 pages and the Accession Code is **BN13654**.

Please note that as part of the production process, APS converts all articles, regardless of their original source, into standardized XML that in turn is used to create the PDF and online versions of the article as well as to populate third-party systems such as Portico, Crossref, and Web of Science. We share our authors' high expectations for the fidelity of the conversion into XML and for the accuracy and appearance of the final, formatted PDF. This process works exceptionally well for the vast majority of articles; however, please check carefully all key elements of your PDF proof, particularly any equations or tables.

Figures submitted electronically as separate files containing color appear in color in the online journal. However, all figures will appear as grayscale images in the print journal unless the color figure charges have been paid in advance, in accordance with our policy for color in print (https://journals.aps.org/authors/color-figures-print).

Specific Questions and Comments to Address for This Paper

1 Please provide ZIP code.
2 Please provide the reference with the label yanagisawa2012gamma3 cited with Refs. [24,25] but not included in the reference list.
3 Please define OP.
4 Please define u-reps.
5 Please define LBCO.
6 As meant to change "falsify" to "disprove" in "further support or falsify this idea"? Please check.
7 Please update Ref. [18] with a published article if possible.
8 Pleae provide publisher's location for Ref. [27].
9 Please verify check in the author name entity- L. P. Pitaevskii in Ref. [27].
Q: This reference could not be uniquely identified due to incomplete information or improper format. Please check all information and amend if applicable.

ORCIDs: Please follow any ORCID links (ⓘ) after the author names and verify that they point to the appropriate record for each author.

Open Funder Registry: Information about an article's funding sources is now submitted to Crossref to help you comply with current or future funding agency mandates. Crossref's Open Funder Registry (https://www.crossref.org/services/funder-registry/) is the definitive registry of funding agencies. Please ensure that your acknowledgments include all sources of funding for your article following any requirements of your funding sources. Where possible, please include grant and award ids. Please carefully check the following funder information we have already extracted from your article and ensure its accuracy and completeness:
NSF (US), DMR-1719490
NSF (US), DMR-1719875
NSF (US), DMR-1752784

Other Items to Check

- Please note that the original manuscript has been converted to XML prior to the creation of the PDF proof, as described above. Please carefully check all key elements of the paper, particularly the equations and tabular data.
- Title: Please check; be mindful that the title may have been changed during the peer-review process.
- Author list: Please make sure all authors are presented, in the appropriate order, and that all names are spelled correctly.
- Please make sure you have inserted a byline footnote containing the email address for the corresponding author, if desired. Please note that this is not inserted automatically by this journal.
- Affiliations: Please check to be sure the institution names are spelled correctly and attributed to the appropriate author(s).
- Receipt date: Please confirm accuracy.
- Acknowledgments: Please be sure to appropriately acknowledge all funding sources.
- Hyphenation: Please note hyphens may have been inserted in word pairs that function as adjectives when they occur before a noun, as in "x-ray diffraction," "4-mm-long gas cell," and "*R*-matrix theory." However, hyphens are deleted from word pairs when they are not used as adjectives before nouns, as in "emission by x rays," "was 4 mm in length," and "the *R* matrix is tested."

  Note also that Physical Review follows U.S. English guidelines in that hyphens are not used after prefixes or before suffixes: superresolution, quasiequilibrium, nanoprecipitates, resonancelike, clockwise.

- Please check that your figures are accurate and sized properly. Make sure all labeling is sufficiently legible. Figure quality in this proof is representative of the quality to be used in the online journal. To achieve manageable file size for online delivery, some compression and downsampling of figures may have occurred. Fine details may have become somewhat fuzzy, especially in color figures. The print journal uses files of higher resolution and therefore details may be sharper in print. Figures to be published in color online will appear in color on these proofs if viewed on a color monitor or printed on a color printer.
- Please check to ensure that reference titles are given as appropriate.
- Overall, please proofread the entire *formatted* article very carefully. The redlined PDF should be used as a guide to see changes that were made during copyediting. However, note that some changes to math and/or layout may not be indicated.

Ways to Respond

- ***Web:*** If you accessed this proof online, follow the instructions on the web page to submit corrections.
- ***Email:*** Send corrections to prbproofs@aptaracorp.com
  Subject: **BN13654** proof corrections
- ***Fax:*** Return this proof with corrections to +1.703.791.1217. Write **Attention:** PRB Project Manager and the Article ID, **BN13654**, on the proof copy unless it is already printed on your proof printout.

PHYSICAL REVIEW B **00**, 005100 (2020)

Elastic properties of hidden order in URu_2Si_2 are reproduced by a staggered nematic

Jaron Kent-Dobias, Michael Matty, and B. J. Ramshaw
Laboratory of Atomic and Solid State Physics, Cornell University, Ithaca, New York, USA

(Received 21 January 2020; revised 3 July 2020; accepted 30 July 2020; published xxxxxxxxxx)

We develop a phenomenological mean-field theory describing the hidden-order phase in URu_2Si_2 as a nematic of the B_{1g} representation staggered along the c axis. Several experimental features are reproduced by this theory: the topology of the temperature-pressure phase diagram, the response of the elastic modulus $(C_{11} - C_{12})/2$ above the transition at ambient pressure, and orthorhombic symmetry breaking in the high-pressure antiferromagnetic phase. In this scenario, hidden order is characterized by broken rotational symmetry that is modulated along the c axis, the primary order of the high-pressure phase is an unmodulated nematic, and the triple point joining those two phases with the high-temperature paramagnetic phase is a Lifshitz point.

DOI: 10.1103/PhysRevB.00.005100

I. INTRODUCTION

URu_2Si_2 is a paradigmatic example of a material with an ordered state whose broken symmetry remains unknown. This state, known as *hidden order* (HO), sets the stage for unconventional superconductivity that emerges at even lower temperatures. At sufficiently large hydrostatic pressures, both superconductivity and HO give way to local moment antiferromagnetism (AFM) [1]. Modern theories [2–19] propose associating any of a variety of broken symmetries with HO. Motivated by the anomalous temperature dependence of one of the elastic moduli, this work analyzes a family of phenomenological models with order parameters of general symmetry that couple linearly to strain. Of these, only one is compatible with two experimental observations: first, the B_{1g} "nematic" elastic susceptibility $(C_{11} - C_{12})/2$ softens anomalously from room temperature down to $T_{\mathrm{HO}} = 17.5$ K [20], and second, a B_{1g} nematic distortion is observed by x-ray scattering under sufficient pressure to destroy the HO state [21].

Recent resonant ultrasound spectroscopy (RUS) measurements were used to examine the thermodynamic discontinuities in the elastic moduli at T_{HO} [22]. The observation of discontinuities only in compressional, or A_{1g}, elastic moduli requires that the point-group representation of HO be one-dimensional. This rules out many order parameter candidates [11–15,19,23] in a model-independent way but does not differentiate between those that remain.

Recent x-ray experiments discovered rotational symmetry breaking in URu_2Si_2 under pressure [21]. Above 0.13–0.5 GPa (depending on temperature), URu_2Si_2 undergoes a B_{1g} nematic distortion, which might be related to the anomalous softening of the B_{1g} elastic modulus $(C_{11} - C_{12})/2$ that occurs over a broad temperature range at zero pressure [24,25]. Motivated by these results—which hint at a B_{1g} strain susceptibility associated with the HO state—we construct a phenomenological mean-field theory for an arbitrary OP coupled to strain and then determine the effect of its phase transitions on the elastic response in different symmetry channels.

We find that only one OP representation reproduces the anomalous B_{1g} elastic modulus, which softens in a Curie-Weiss-like manner from room temperature and then cusps at T_{HO}. That theory associates HO with a B_{1g} OP modulated along the c axis, the high-pressure state with uniform B_{1g} order, and the triple point between them with a Lifshitz point. In addition to the agreement with the ultrasound data across a broad temperature range, our model predicts uniform B_{1g} strain at high pressure—the same distortion that was recently seen in x-ray scattering experiments [21]. This work strongly motivates future ultrasound experiments under pressure approaching the Lifshitz point, which should find that the $(C_{11} - C_{12})/2$ modulus diverges as the uniform B_{1g} strain of the high-pressure phase is approached.

II. MODEL AND PHASE DIAGRAM

The point group of URu_2Si_2 is D_{4h}, and any theory must locally respect this symmetry in the high-temperature phase. Our phenomenological free-energy density contains three parts: the elastic free energy, the OP, and the interaction between strain and OP. The most general quadratic free energy of the strain ϵ is $f_{\mathrm{ELASTIC}} = C^0_{ijkl}\epsilon_{ij}\epsilon_{kl}$ [26]. The form of the bare moduli tensor C^0 is further restricted by symmetry [27]. Linear combinations of the six independent components of strain form five irreducible components of strain in D_{4h} as

$$\epsilon_{A_{1g},1} = \epsilon_{11} + \epsilon_{22}, \quad \epsilon_{B_{1g}} = \epsilon_{11} - \epsilon_{22}, \quad \epsilon_{A_{1g},2} = \epsilon_{33},$$
$$\epsilon_{B_{2g}} = 2\epsilon_{12}, \quad \epsilon_{E_g} = 2\{\epsilon_{11}, \epsilon_{22}\}. \tag{1}$$

All quadratic combinations of these irreducible strains that transform like A_{1g} are included in the free energy,

$$f_{\mathrm{ELASTIC}} = \frac{1}{2}\sum_{\mathrm{X}} C^0_{\mathrm{X},ij}\epsilon_{\mathrm{X},i}\epsilon_{\mathrm{X},j}, \tag{2}$$

where the sum is over irreducible representations (irreps) of the point group and the bare elastic moduli C^0_X are

$$C^0_{A_{1g},11} = \tfrac{1}{2}\big(C^0_{1111} + C^0_{1122}\big), \quad C^0_{B_{1g}} = \tfrac{1}{2}\big(C^0_{1111} - C^0_{1122}\big),$$
$$C^0_{A_{1g},22} = C^0_{3333}, \quad C^0_{B_{2g}} = C^0_{1212}, \quad C^0_{A_{1g},12} = C^0_{1133},$$
$$C^0_{E_g} = C^0_{1313}. \tag{3}$$

The interaction between strain and an OP η depends on the point-group representation of η. If this representation is X, the most general coupling to linear order is

$$f_{\text{INT}} = -b^{(i)}\epsilon^{(i)}_X \eta. \tag{4}$$

Many high-order interactions are permitted, and in the Appendix another of the form $\epsilon^2\eta^2$ is added to the following analysis. If there exists no component of strain that transforms like the representation X then there can be no linear coupling. The next-order coupling is linear in strain and quadratic in order parameter, and the effect of this coupling at a continuous phase transition is to produce a jump in the A_{1g} elastic moduli if η is single component [28–30] and jumps in other elastic moduli if it is multicomponent [22]. Because we are interested in physics that anticipates the phase transition—for instance, that the growing OP susceptibility is reflected directly in the elastic susceptibility—we will focus our attention on OPs that can produce linear couplings to strain. Looking at the components present in (1), this rules out all of the u-reps (which are odd under inversion), the A_{2g} irrep, and all half-integer (spinor) representations.

If the OP transforms like A_{1g} (e.g., a fluctuation in valence number), odd terms are allowed in its free energy and without fine-tuning any transition will be first order and not continuous. Since the HO phase transition is second order [20], we will henceforth rule out A_{1g} OPs as well. For the OP representation X as any of those remaining—B_{1g}, B_{2g}, or E_g—the most general quadratic free-energy density is

$$f_{\text{OP}} = \tfrac{1}{2}\big[r\eta^2 + c_\parallel(\nabla_\parallel\eta)^2 + c_\perp(\nabla_\perp\eta)^2 + D_\perp\big(\nabla^2_\perp\eta\big)^2\big] + u\eta^4, \tag{5}$$

where $\nabla_\parallel = \{\partial_1, \partial_2\}$ transforms like E_u and $\nabla_\perp = \partial_3$ transforms like A_{2u}. Other quartic terms are allowed—especially many for an E_g OP—but we have included only those terms necessary for stability when either r or $c_\perp$ becomes negative as a function of temperature. The full free-energy functional of η and ϵ is

$$F[\eta,\epsilon] = F_{\text{OP}}[\eta] + F_{\text{ELASTIC}}[\epsilon] + F_{\text{INT}}[\eta,\epsilon] = \int dx\,(f_{\text{OP}} + f_{\text{ELASTIC}} + f_{\text{INT}}). \tag{6}$$

Rather than analyze this two-argument functional directly, we begin by tracing out the strain and studying the behavior of the OP alone. Later, we will invert this procedure and trace out the OP when we compute the effective elastic moduli. The only strain relevant to an OP of representation X at linear coupling is ϵ_X, which can be traced out of the problem exactly in mean-field theory. Extremizing the functional (6) with respect to ϵ_X gives

$$0 = \left.\frac{\delta F[\eta,\epsilon]}{\delta\epsilon_X(x)}\right|_{\epsilon=\epsilon_\star} = C^0_X\epsilon^\star_X(x) - b\eta(x), \tag{7}$$

which in turn gives the strain field conditioned on the state of the OP field as $\epsilon^\star_X[\eta](x) = (b/C^0_X)\eta(x)$ at all spatial coordinates x and $\epsilon^\star_Y[\eta] = 0$ for all other irreps $Y \neq X$. Upon substitution into (6), the resulting single-argument free-energy functional $F[\eta,\epsilon_\star[\eta]]$ has a density identical to f_{OP} with the identification $r \to \tilde{r} = r - b^2/2C^0_X$.

With the strain traced out, (5) describes the theory of a Lifshitz point at $\tilde{r} = c_\perp = 0$ [31,32]. The properties discussed in the remainder of this section can all be found in a standard text (e.g., [33]). For a one-component OP (B_{1g} or B_{2g}) and positive $c_\parallel$, it is traditional to make the field ansatz $\langle\eta(x)\rangle = \eta_*\cos(q_*x_3)$. For $\tilde{r} > 0$ and $c_\perp > 0$ or $\tilde{r} > c^2_\perp/4D_\perp$ and $c_\perp < 0$, the only stable solution is $\eta_* = q_* = 0$, and the system is unordered. For $\tilde{r} < 0$ there are free-energy minima for $q_* = 0$ and $\eta^2_* = -\tilde{r}/4u$, and this system has uniform order of the OP representation, e.g., B_{1g} or B_{2g}. For $c_\perp < 0$ and $\tilde{r} < c^2_\perp/4D_\perp$ there are free-energy minima for $q^2_* = -c_\perp/2D_\perp$ and

$$\eta^2_* = \frac{c^2_\perp - 4D_\perp\tilde{r}}{12D_\perp u} = \frac{\tilde{r}_c - \tilde{r}}{3u} = \frac{|\Delta\tilde{r}|}{3u}, \tag{8}$$

with $\tilde{r}_c = c^2_\perp/4D_\perp$, and the system has modulated order. The transition between the uniform and modulated orderings is first order for a one-component OP and occurs along the line $c_\perp = -2\sqrt{-D_\perp\tilde{r}/5}$.

For a two-component OP (E_g) we must also allow a relative phase between the two components of the OP. In this case the uniform ordered phase is stable only for $c_\perp > 0$, and the modulated phase is now characterized by helical order with $\langle\eta(x)\rangle = \eta_*\{\cos(q_*x_3), \sin(q_*x_3)\}$. The uniform to modulated transition is now continuous. This does not reproduce the physics of URu_2Si_2, whose HO phase is bounded by a line of first-order transitions at high pressure, and so we will henceforth neglect the possibility of a multicomponent order parameter—consistent with earlier ultrasound measurements [22]. Schematic phase diagrams for both the one- and two-component models are shown in Fig. 1.

III. SUSCEPTIBILITY AND ELASTIC MODULI

We will now derive the effective elastic tensor C that results from the coupling of strain to the OP. The ultimate result, found in (17), is that C_X differs from its bare value C^0_X only for the representation X of the OP. Moreover, this modulus does not vanish at the unordered to modulated transition—as it would if the transition were a $q = 0$ phase transition—but instead ends in a cusp. In this section we start by computing the susceptibility of the OP at the unordered to modulated transition and then compute the elastic modulus for the same.

The susceptibility of a single-component (B_{1g} or B_{2g}) OP is

$$\chi^{\{-1\}}(x,x') = \left.\frac{\delta^2 F[\eta,\epsilon_\star[\eta]]}{\delta\eta(x)\delta\eta(x')}\right|_{\eta=\langle\eta\rangle} = \big[\tilde{r} - c_\parallel\nabla^2_\parallel - c_\perp\nabla^2_\perp + D_\perp\nabla^4_\perp + 12u\langle\eta(x)\rangle^2\big] \times \delta(x-x'), \tag{9}$$

where $\{-1\}$ indicates a functional reciprocal defined as

$$\int dx''\,\chi^{\{-1\}}(x,x'')\chi(x'',x') = \delta(x-x'). \tag{10}$$

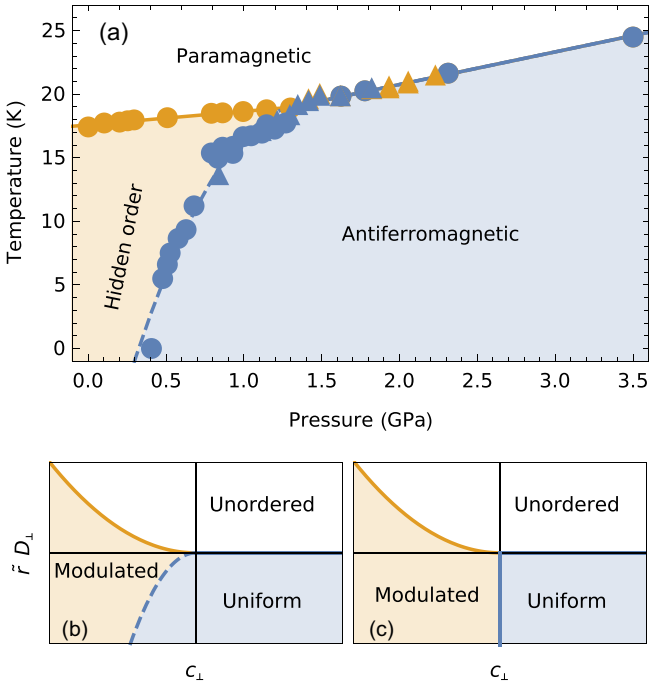

FIG. 1. Phase diagrams for (a) URu_2Si_2 from experiments (neglecting the superconducting phase) [1], (b) mean-field theory of a one-component (B_{1g} or B_{2g}) Lifshitz point, and (c) mean-field theory of a two-component (E_g) Lifshitz point. Solid lines denote second-order transitions, while dashed lines denote first-order transitions. Later, when we fit the elastic moduli predictions for a B_{1g} OP to data along the ambient pressure line, we will take $\Delta\tilde{r} = \tilde{r} - \tilde{r}_c = a(T - T_c)$.

Taking the Fourier transform and integrating out q' give

$$\chi(q) = \left(\tilde{r} + c_\parallel q_\parallel^2 + c_\perp q_\perp^2 + D_\perp q_\perp^4 + 12u \sum_{q'} \langle \tilde{\eta}_{q'} \rangle \langle \tilde{\eta}_{-q'} \rangle\right)^{-1}. \tag{11}$$

Near the unordered to modulated transition this yields

$$\begin{aligned}\chi(q) &= \left[c_\parallel q_\parallel^2 + D_\perp\left(q_*^2 - q_\perp^2\right)^2 + |\Delta\tilde{r}|\right]^{-1} \\ &= \frac{1}{D_\perp}\frac{\xi_\perp^4}{1 + \xi_\parallel^2 q_\parallel^2 + \xi_\perp^4\left(q_*^2 - q_\perp^2\right)^2},\end{aligned} \tag{12}$$

with $\xi_\perp = (|\Delta\tilde{r}|/D_\perp)^{-1/4} = \xi_{\perp 0}|t|^{-1/4}$ and $\xi_\parallel = (|\Delta\tilde{r}|/c_\parallel)^{-1/2} = \xi_{\parallel 0}|t|^{-1/2}$, where $t = (T - T_c)/T_c$ is the reduced temperature and $\xi_{\perp 0} = (D_\perp/aT_c)^{1/4}$ and $\xi_{\parallel 0} = (c_\parallel/aT_c)^{1/2}$ are the bare correlation lengths perpendicular and parallel to the plane, respectively. The static susceptibility $\chi(0) = (D_\perp q_*^4 + |\Delta\tilde{r}|)^{-1}$ does not diverge at the unordered to modulated transition. Although it anticipates a transition with Curie-Weiss-like divergence at the lower point $a(T - T_c) = \Delta\tilde{r} = -D_\perp q_*^4 < 0$, this is cut off with a cusp at the phase transition at $\Delta\tilde{r} = 0$.

The elastic susceptibility, which is the reciprocal of the effective elastic modulus, is found in a way similar to the OP susceptibility: we must trace over η and take the second variation of the resulting effective free-energy functional of ϵ alone. Extremizing over η yields

$$0 = \left.\frac{\delta F[\eta,\epsilon]}{\delta\eta(x)}\right|_{\eta=\eta_\star} = \left.\frac{\delta F_{\rm OP}[\eta]}{\delta\eta(x)}\right|_{\eta=\eta_\star} - b\epsilon_{\rm X}(x), \tag{13}$$

which implicitly gives $\eta_\star[\epsilon]$, the OP conditioned on the configuration of the strain. Since $\eta_\star$ is a functional of $\epsilon_{\rm X}$ alone, only the modulus $C_{\rm X}$ will be modified from its bare value $C_{\rm X}^0$.

Although the differential equation for $\eta_\star$ cannot be solved explicitly, we can use the inverse function theorem to make use of (13) anyway. First, denote by $\eta_\star^{-1}[\eta]$ the inverse functional of $\eta_\star$ implied by (13), which gives the function $\epsilon_{\rm X}$ corresponding to each solution of (13) it receives. This we can immediately identify from (13) as $\eta_\star^{-1}[\eta](x) = b^{-1}\{\delta F_{\rm OP}[\eta]/\delta\eta(x)\}$. Now, we use the inverse function theorem to relate the functional reciprocal of the derivative of $\eta_\star[\epsilon]$ with respect to $\epsilon_{\rm X}$ to the derivative of $\eta_\star^{-1}[\eta]$ with respect to η, yielding

$$\begin{aligned}\left(\frac{\delta\eta_\star[\epsilon](x)}{\delta\epsilon_{\rm X}(x')}\right)^{\{-1\}} &= \left.\frac{\delta\eta_\star^{-1}[\eta](x)}{\delta\eta(x')}\right|_{\eta=\eta_\star[\epsilon]} \\ &= b^{-1}\left.\frac{\delta^2 F_{\rm OP}[\eta]}{\delta\eta(x)\delta\eta(x')}\right|_{\eta=\eta_\star[\epsilon]}.\end{aligned} \tag{14}$$

Next, (13) and (14) can be used in concert with the ordinary rules of functional calculus to yield the second variation

$$\begin{aligned}\frac{\delta^2 F[\eta_\star[\epsilon],\epsilon]}{\delta\epsilon_{\rm X}(x)\delta\epsilon_{\rm X}(x')} &= C_{\rm X}^0\delta(x-x') - 2b\frac{\delta\eta_\star[\epsilon](x)}{\delta\epsilon_{\rm X}(x')} - b\int dx''\,\frac{\delta^2\eta_\star[\epsilon](x)}{\delta\epsilon_{\rm X}(x')\delta\epsilon_{\rm X}(x'')}\epsilon_{\rm X}(x'') \\ &\quad + \int dx''\,\frac{\delta^2\eta_\star[\epsilon](x'')}{\delta\epsilon_{\rm X}(x)\delta\epsilon_{\rm X}(x')}\left.\frac{\delta F_{\rm OP}[\eta]}{\delta\eta(x'')}\right|_{\eta=\eta_\star[\epsilon]} + \int dx''\,dx'''\,\frac{\delta\eta_\star[\epsilon](x'')}{\delta\epsilon_{\rm X}(x)}\frac{\delta\eta_\star[\epsilon](x''')}{\delta\epsilon_{\rm X}(x')}\left.\frac{\delta^2 F_{\rm OP}[\eta]}{\delta\eta(x'')\delta\eta(x''')}\right|_{\eta=\eta_\star[\epsilon]} \\ &= C_{\rm X}^0\delta(x-x') - 2b\frac{\delta\eta_\star[\epsilon](x)}{\delta\epsilon_{\rm X}(x')} - b\int dx''\,\frac{\delta^2\eta_\star[\epsilon](x)}{\delta\epsilon_{\rm X}(x')\delta\epsilon_{\rm X}(x'')}\epsilon_{\rm X}(x'') \\ &\quad + \int dx''\,\frac{\delta^2\eta_\star[\epsilon](x'')}{\delta\epsilon_{\rm X}(x)\delta\epsilon_{\rm X}(x')}[b\epsilon_{\rm X}(x'')] + b\int dx''\,dx'''\,\frac{\delta\eta_\star[\epsilon](x'')}{\delta\epsilon_{\rm X}(x)}\frac{\delta\eta_\star[\epsilon](x''')}{\delta\epsilon_{\rm X}(x')}\left(\frac{\partial\eta_\star[\epsilon](x'')}{\partial\epsilon_{\rm X}(x''')}\right)^{\{-1\}} \\ &= C_{\rm X}^0\delta(x-x') - 2b\frac{\delta\eta_\star[\epsilon](x)}{\delta\epsilon_{\rm X}(x')} + b\int dx''\,\delta(x-x'')\frac{\delta\eta_\star[\epsilon](x'')}{\delta\epsilon_{\rm X}(x')} = C_{\rm X}^0\delta(x-x') - b\frac{\delta\eta_\star[\epsilon](x)}{\delta\epsilon_{\rm X}(x')}.\end{aligned} \tag{15}$$

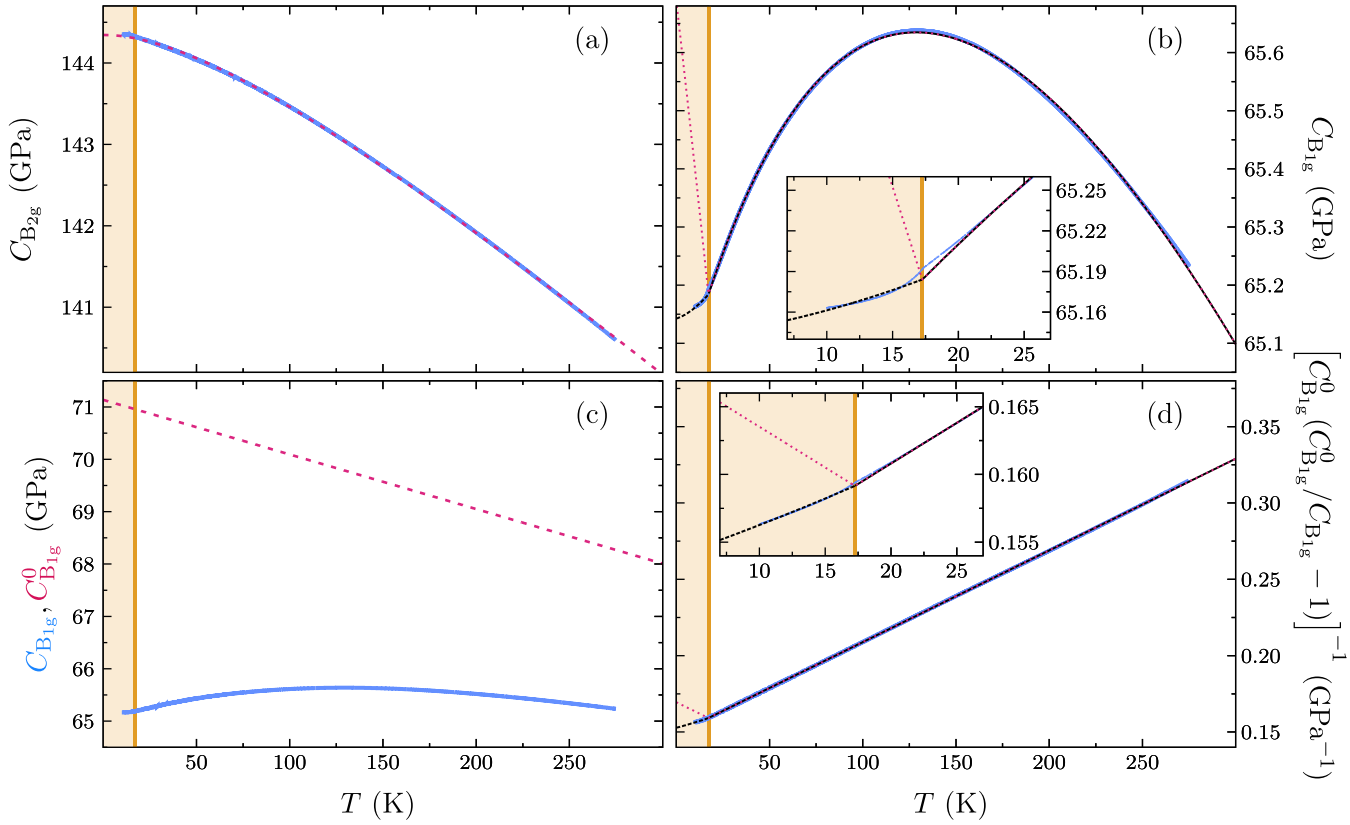

FIG. 2. RUS measurements of the elastic moduli of URu_2Si_2 at ambient pressure as a function of temperature from recent experiments [22] (blue solid line) alongside fits to theory (magenta dashed and black dashed lines). The solid yellow region shows the location of the HO phase. (a) B_{2g} modulus data and a fit to the standard form [34]. (b) B_{1g} modulus data and a fit to (18) (magenta dashed line) and a fit to (A21) (black dashed line). The fit gives $C^0_{B_{1g}} \simeq [71 - (0.010\,\mathrm{K}^{-1})T]$ GPa, $b^2/D_\perp q_*^4 \simeq 6.28$ GPa, and $b^2/a \simeq 1665$ GPa K^{-1}. Addition of a quadratic term in $C^0_{B_{1g}}$ was not needed here for the fit [34]. (c) B_{1g} modulus data and the fit of the *bare* B_{1g} modulus. (d) B_{1g} modulus data and the fits transformed by $[C^0_{B_{1g}}(C^0_{B_{1g}}/C_{B_{1g}} - 1)]^{-1}$, which is predicted from (18) to equal $D_\perp q_*^4/b^2 + a/b^2|T - T_c|$, e.g., an absolute-value function.

The elastic modulus is given by the second variation (15) evaluated at the extremized strain $\langle\epsilon\rangle$. To calculate it, note that evaluating the second variation of F_{OP} in (14) at $\langle\epsilon\rangle$ (or $\eta_\star(\langle\epsilon\rangle) = \langle\eta\rangle$) yields

$$\left(\frac{\delta\eta_\star[\epsilon](x)}{\delta\epsilon_{\mathrm{X}}(x')}\right)^{\{-1\}}\Bigg|_{\epsilon=\langle\epsilon\rangle} = b^{-1}\chi^{\{-1\}}(x,x') + \frac{b}{C^0_{\mathrm{X}}}\delta(x-x'), \tag{16}$$

where $\chi^{\{-1\}}$ is the OP susceptibility given by (9). Upon substitution into (15) and taking the Fourier transform of the result, we finally arrive at

$$C_{\mathrm{X}}(q) = C^0_{\mathrm{X}} - b\left(\frac{1}{b\chi(q)} + \frac{b}{C^0_{\mathrm{X}}}\right)^{-1} = C^0_{\mathrm{X}}\left(1 + \frac{b^2}{C^0_{\mathrm{X}}}\chi(q)\right)^{-1}. \tag{17}$$

Although not relevant here, this result generalizes to multicomponent OPs.

What does (17) predict in the vicinity of the HO transition? Near the disordered-to-modulated transition—the zero-pressure transition to the HO state—the static modulus is given by

$$C_{\mathrm{X}}(0) = C^0_{\mathrm{X}}\left[1 + \frac{b^2}{C^0_{\mathrm{X}}}(D_\perp q_*^4 + |\Delta\tilde{r}|)^{-1}\right]^{-1}. \tag{18}$$

This corresponds to a softening in the X modulus approaching the transition that is cut off with a cusp of the form $|\Delta\tilde{r}|^\gamma \propto |T - T_c|^\gamma$, with $\gamma = 1$. This is our main result. The only OP irreps that couple linearly with strain and reproduce the topology of the URu_2Si_2 phase diagram are B_{1g} and B_{2g}. For either of these irreps, the transition into a modulated rather than uniform phase masks traditional signatures of a continuous transition by locating thermodynamic singularities at nonzero $q = q_*$. The remaining clue at $q = 0$ is a particular kink in the corresponding modulus.

IV. COMPARISON TO EXPERIMENT

RUS experiments [22] yield the individual elastic moduli broken into irreps; data for the B_{1g} and B_{2g} components defined in (1) are shown in Figs. 2(a) and 2(b). The B_{2g} modulus in Fig. 2(a) does not appear to have any response to the presence of the transition, exhibiting the expected linear stiffening upon cooling from room temperature, with a low-temperature cutoff at some fraction of the Debye temperature [34]. The B_{1g} modulus in Fig. 2(b) has a dramatic response, softening over the course of roughly 100 K and then cusping at the HO transition. The data in the high-temperature phase can be fit

to the theory (18), with a linear background modulus $C^0_{B_{1g}}$ and $\tilde{r} - \tilde{r}_c = a(T - T_c)$, and the result is shown in Fig. 2(b).

The behavior of the modulus below the transition does not match (18) well, but this is because of the truncation of the free-energy expansion used above. Higher-order terms like $\eta^2\epsilon^2$ and ϵ^4 contribute to the modulus starting at order η_*^2 and therefore change the behavior below the transition, where the expectation value of η is finite, but not above it, where the expectation value of η is zero. To demonstrate this, in the Appendix we compute the modulus in a theory where the interaction free energy is truncated after fourth order with the new term $\frac{1}{2}g\eta^2\epsilon^2$. The dashed black line in Fig. 2 shows the fit of the RUS data to (A21) and shows that successive high-order corrections can account for the low-temperature behavior.

The data and theory appear quantitatively consistent, suggesting that HO can be described as a B_{1g}-nematic phase that is modulated at finite q along the c axis. The predicted softening appears over hundreds of kelvins; Figs. 2(c) and 2(d) show the background modulus $C^0_{B_{1g}}$ and the OP-induced response isolated from each other.

We have seen that the mean-field theory of a B_{1g} OP recreates the topology of the HO phase diagram and the temperature dependence of the B_{1g} elastic modulus at zero pressure. This theory has several other physical implications. First, the association of a modulated B_{1g} order with the HO phase implies a *uniform* B_{1g} order associated with the high-pressure phase and, moreover, a uniform B_{1g} strain of magnitude $\langle\epsilon_{B_{1g}}\rangle^2 = b^2\tilde{r}/4u(C^0_{B_{1g}})^2$, which corresponds to an orthorhombic structural phase. The onset of orthorhombic symmetry breaking was recently detected at high pressure in URu_2Si_2 using x-ray diffraction, a further consistency of this theory with the phenomenology of URu_2Si_2[21].

Second, as the Lifshitz point is approached from low pressure, this theory predicts that the modulation wave vector q_* should vanish continuously. Far from the Lifshitz point we expect the wave vector to lock into values commensurate with the space group of the lattice and, moreover, that at zero pressure, where the RUS data here were collected, the half-wavelength of the modulation should be commensurate with the lattice spacing $a_3 \simeq 9.68$ Å, or $q_* = \pi/a_3 \simeq 0.328$ Å^{-1} [35–42]. In between these two regimes, mean-field theory predicts that the ordering wave vector shrinks by jumping between ever-closer commensurate values in the style of the devil's staircase [43]. In reality the presence of fluctuations may wash out these transitions.

This motivates future ultrasound experiments done under pressure, where the depth of the cusp in the B_{1g} modulus should deepen (perhaps with these commensurability jumps) at low pressure and approach zero as $q_*^4 \sim (c_\perp/2D_\perp)^2$ near the Lifshitz point. Alternatively, RUS done at ambient pressure might examine the heavy Fermi liquid to AFM transition by doping. Although previous RUS studies have doped URu_2Si_2 with rhodium [44], rhodium changes the carrier concentration as well as the lattice spacing and may favor the promotion of the magnetic phase. An isoelectronic (as well as isomagnetic) dopant such as iron may more faithfully explore the transition out of the HO phase. Our work also motivates experiments that can probe the entire correlation function—like x-ray and neutron scattering—and directly resolve its finite-q divergence. The presence of spatial commensurability is known to be irrelevant to critical behavior at a one-component disordered-to-modulated transition and therefore is not expected to modify the thermodynamic behavior otherwise [45].

There are two apparent discrepancies between the orthorhombic strain in the phase diagram presented by recent x-ray data [21] and that predicted by our mean-field theory if its uniform B_{1g} phase is taken to be coincident with URu_2Si_2's AFM. The first is the apparent onset of the orthorhombic phase in the HO state at slightly lower pressures than the onset of AFM. As recent x-ray research [21] notes, this misalignment of the two transitions as a function of doping could be due to the lack of an ambient pressure calibration for the lattice constant. The second discrepancy is the onset of orthorhombicity at higher temperatures than the onset of AFM. We note that magnetic susceptibility data see no trace of another phase transition at these higher temperatures [46]. It is therefore possible that the high-temperature orthorhombic signature in x-ray scattering is not the result of a bulk thermodynamic phase but, instead, marks the onset of short-range correlations, as it does in the high-T_c cuprates [47] (where the onset of the charge density wave correlations also lacks a thermodynamic phase transition).

Three dimensions is below the upper critical dimension $4\frac{1}{2}$ of a one-component disordered-to-modulated transition, and so mean-field theory should break down sufficiently close to the critical point due to fluctuations at the Ginzburg temperature [48,49]. Magnetic phase transitions tend to have a Ginzburg temperature of order 1. Our fit above gives $\xi_{\perp 0}q_* = (D_\perp q_*^4/aT_c)^{1/4} \simeq 2$, which combined with the speculation of $q_* \simeq \pi/a_3$ puts the bare correlation length $\xi_{\perp 0}$ on the order of lattice constant, which is about what one would expect for a generic magnetic transition. The agreement of these data in the $(T - T_{HO})/T_{HO} \sim 0.1$–10 range with the mean-field exponent suggests that this region is outside the Ginzburg region, but an experiment may begin to see deviations from mean-field behavior within approximately several kelvins of the critical point. An ultrasound experiment with finer temperature resolution near the critical point may be able to resolve a modified cusp exponent $\gamma \simeq 1.31$ [50] since, according to one analysis, the universality class of a uniaxial modulated one-component OP is that of the O(2), three-dimensional XY transition [45]. A crossover from mean-field theory may explain the small discrepancy in our fit very close to the critical point.

V. CONCLUSION AND OUTLOOK

We have developed a general phenomenological treatment of HO OPs that have the potential for linear coupling to strain. The two representations with mean-field phase diagrams that are consistent with the phase diagram of URu_2Si_2 are B_{1g} and B_{2g}. Of these, only a staggered B_{1g} OP is consistent with zero-pressure RUS data, with a cusp appearing in the associated elastic modulus. In this picture, the HO phase is characterized by uniaxial modulated B_{1g} order, while the high-pressure phase is characterized by uniform B_{1g} order. The staggered nematic of HO is similar to the striped superconducting phase found in LBCO and other cuprates [51].

We can also connect our results to the large body of work concerning various multipolar orders as candidate states for HO (e.g., Refs. [3–5,7–9]). Physically, our phenomenological order parameter could correspond to B_{1g} multipolar ordering originating from the localized component of the U $5f$ electrons. For the crystal field states of URu_2Si_2, this could correspond either to electric quadrupolar or hexadecapolar order based on the available multipolar operators [4].

The coincidence of our theory's orthorhombic high-pressure phase and URu_2Si_2's AFM is compelling, but our mean-field theory does not make any explicit connection with the physics of AFM. Neglecting this physics could be reasonable since correlations often lead to AFM as a secondary effect, like what occurs in many Mott insulators. An electronic theory of this phase diagram may find that the AFM observed in URu_2Si_2 indeed follows along with an independent high-pressure orthorhombic phase associated with uniform B_{1g} electronic order.

The corresponding prediction of uniform B_{1g} symmetry breaking in the high-pressure phase is consistent with recent diffraction experiments [21], except for the apparent earlier onset in temperature of the B_{1g} symmetry breaking, which we believe may be due to fluctuating order at temperatures above the actual transition temperature. This work motivates both further theoretical work regarding a microscopic theory with modulated B_{1g} order and preforming symmetry-sensitive thermodynamic experiments at pressure, such as pulse-echo ultrasound, that could further support or disprove this idea.

ACKNOWLEDGMENTS

J.K.-D. is supported by NSF Grant No. DMR-1719490, M.M. is supported by NSF Grant No. DMR-1719875, and B.J.R. is supported by NSF Grant No. DMR-1752784. We are grateful for helpful discussions with S. Raghu, S. Kivelson, D. Liarte, and J. Sethna and for permission to reproduce experimental data in our figure by E. Hassinger. We thank S. Ghosh for RUS data.

APPENDIX: ADDING A HIGHER-ORDER INTERACTION

In this Appendix, we compute the B_{1g} modulus for a theory with a high-order interaction truncation to better match the low-temperature behavior. Consider the free-energy density $f = f_{\text{ELASTIC}} + f_{\text{INT}} + f_{\text{OP}}$, with

$$f_{\text{ELASTIC}} = \tfrac{1}{2}C_0\epsilon^2, \quad f_{\text{INT}} = -b\epsilon\eta + \tfrac{1}{2}g\epsilon^2\eta^2, \quad f_{\text{OP}} = \tfrac{1}{2}\left[r\eta^2 + c_{\parallel}(\nabla_{\parallel}\eta)^2 + c_{\perp}(\nabla_{\perp}\eta)^2 + D\left(\nabla_{\perp}^2\eta\right)^2\right] + u\eta^4. \tag{A1}$$

The mean-field strain conditioned on the order parameter is found from

$$= \left.\frac{\delta F[\eta,\epsilon]}{\delta\epsilon(x)}\right|_{\epsilon=\epsilon_\star[\eta]} = C_0\epsilon_\star[\eta](x) - b\eta(x) + g\epsilon_\star[\eta](x)\eta(x)^2, \tag{A2}$$

which yields

$$\epsilon_\star[\eta](x) = \frac{b\eta(x)}{C_0 + g\eta(x)^2}. \tag{A3}$$

Upon substitution into (A1) and expanded to fourth order in η, $F[\eta,\epsilon_\star[\eta]]$ can be written in the form $F_{\text{OP}}[\eta]$ alone with $r \to \tilde{r} = r - b^2/C_0$ and $u \to \tilde{u} = u + b^2g/2C_0^2$. The phase diagram in η follows as before with the shifted coefficients, namely, $\langle\eta(x)\rangle = \eta_*\cos(q_*x_3)$ for $\tilde{r} < c_\perp^2/4D = \tilde{r}_c$, with $q_*^2 = -c_\perp/2D$, and

$$\eta_*^2 = \frac{c_\perp^2 - 4D\tilde{r}}{12D\tilde{u}} = \frac{|\Delta\tilde{r}|}{3\tilde{u}}. \tag{A4}$$

We would like to calculate the q-dependent modulus

$$C(q) = \frac{1}{V}\int dx\,dx'\,C(x,x')e^{-iq(x-x')}, \tag{A5}$$

where

$$C(x,x') = \left.\frac{\delta^2F[\eta_\star[\epsilon],\epsilon]}{\delta\epsilon(x)\delta\epsilon(x')}\right|_{\epsilon=\langle\epsilon\rangle} = \frac{\delta^2F_{\text{ELASTIC}}[\eta_\star[\epsilon],\epsilon]}{\delta\epsilon(x)\delta\epsilon(x')} + \frac{\delta^2F_{\text{INT}}[\eta_\star[\epsilon],\epsilon]}{\delta\epsilon(x)\delta\epsilon(x')} + \left.\frac{\delta^2F_{\text{OP}}[\eta_\star[\epsilon],\epsilon]}{\delta\epsilon(x)\delta\epsilon(x')}\right|_{\epsilon=\langle\epsilon\rangle} \tag{A6}$$

and $\eta_\star$ is the mean-field order parameter conditioned on the strain defined implicitly by

$$0 = \left.\frac{\delta F[\eta,\epsilon]}{\delta\eta(x)}\right|_{\eta=\eta_\star[\epsilon]} = -b\epsilon(x) + g\epsilon(x)^2\eta_\star[\epsilon](x) + \left.\frac{\delta F_{\text{OP}}[\eta]}{\delta\eta(x)}\right|_{\eta=\eta_\star[\epsilon]}. \tag{A7}$$

We will work this out term by term. The elastic term is the most straightforward, giving

$$\frac{\delta^2F_{\text{ELASTIC}}[\epsilon]}{\delta\epsilon(x)\delta\epsilon(x')} = \frac{1}{2}C_0\frac{\delta^2}{\delta\epsilon(x)\delta\epsilon(x')}\int dx''\,\epsilon(x'')^2 = C_0\delta(x-x'). \tag{A8}$$

The interaction term gives

$$\begin{aligned}\frac{\delta^2 F_{\rm INT}[\eta_\star[\epsilon],\epsilon]}{\delta\epsilon(x)\delta\epsilon(x')} &= -b\frac{\delta^2}{\delta\epsilon(x)\delta\epsilon(x')}\int dx''\,\epsilon(x'')\eta_\star[\epsilon](x'') + \frac{1}{2}g\frac{\delta^2}{\delta\epsilon(x)\delta\epsilon(x')}\int dx''\,\epsilon(x'')^2\eta_\star[\epsilon](x'')^2\\ &= -b\frac{\delta\eta_\star[\epsilon](x')}{\delta\epsilon(x)} - b\frac{\delta}{\delta\epsilon(x)}\int dx''\,\epsilon(x'')\frac{\delta\eta_\star[\epsilon](x'')}{\delta\epsilon(x')} + g\frac{\delta}{\delta\epsilon(x)}\{\epsilon(x')\eta_\star[\epsilon](x')^2\}\\ &\quad + g\frac{\delta}{\delta\epsilon(x)}\int dx''\,\epsilon(x'')^2\eta_\star[\epsilon](x'')\frac{\delta\eta_\star[\epsilon](x'')}{\delta\epsilon(x')}\\ &= -2\{b-2g\epsilon(x)\eta_\star[\epsilon](x)\}\frac{\delta\eta_\star[\epsilon](x)}{\delta\epsilon(x')} - b\int dx''\,\epsilon(x'')\frac{\delta^2\eta_\star[\epsilon](x'')}{\delta\epsilon(x)\delta\epsilon(x')} + g\eta_\star[\epsilon](x)^2\delta(x-x')\\ &\quad + g\int dx''\,\epsilon(x'')^2\frac{\delta\eta_\star[\epsilon](x'')}{\delta\epsilon(x)}\frac{\delta\eta_\star[\epsilon](x'')}{\delta\epsilon(x')} + g\int dx''\,\epsilon(x'')^2\eta_\star[\epsilon](x'')\frac{\delta^2\eta_\star[\epsilon](x'')}{\delta\epsilon(x)\delta\epsilon(x')}.\end{aligned} \tag{A9}$$

The order parameter term relies on some other identities. First, (A7) implies

$$\left.\frac{\delta F_{\rm OP}[\eta]}{\delta\eta(x)}\right|_{\eta=\eta_\star[\epsilon]} = b\epsilon(x) - g\epsilon(x)^2\eta_\star[\epsilon](x) \tag{A10}$$

and therefore that the functional inverse $\eta_\star^{-1}[\eta]$ is

$$\eta_\star^{-1}[\eta](x) = \frac{b}{2g\eta(x)}\left(1-\sqrt{1-\frac{4g\eta(x)}{b^2}\frac{\delta F_{\rm OP}[\eta]}{\delta\eta(x)}}\right). \tag{A11}$$

The inverse function theorem further implies [with substitution of (A10) after the derivative is evaluated] that

$$\left(\frac{\delta\eta_\star[\epsilon](x)}{\delta\epsilon(x')}\right)^{\{-1\}} = \left.\frac{\delta\eta_\star^{-1}[\eta](x)}{\delta\eta(x')}\right|_{\eta=\eta_\star[\epsilon]} = \frac{g\epsilon(x)^2\delta(x-x') + \left.\frac{\delta^2 F_{\rm OP}[\eta]}{\delta\eta(x)\delta\eta(x')}\right|_{\eta=\eta_\star[\epsilon]}}{b-2g\epsilon(x)\eta_\star[\epsilon](x)} \tag{A12}$$

and therefore that

$$\left.\frac{\delta^2 F_{\rm OP}[\eta]}{\delta\eta(x)\delta\eta(x')}\right|_{\eta=\eta_\star[\epsilon]} = \{b-2g\epsilon(x)\eta_\star[\epsilon](x)\}\left(\frac{\delta\eta_\star[\epsilon](x)}{\delta\epsilon(x')}\right)^{\{-1\}} - g\epsilon(x)^2\delta(x-x'). \tag{A13}$$

Finally, we evaluate the order parameter term, using (A10) and (A13), which give

$$\begin{aligned}\frac{\delta^2 F_{\rm OP}[\eta_\star[\epsilon]]}{\delta\epsilon(x)\delta\epsilon(x')} &= \frac{\delta}{\delta\epsilon(x)}\int dx''\,\frac{\delta\eta_\star[\epsilon](x'')}{\delta\epsilon(x')}\left.\frac{\delta F_{\rm OP}[\eta]}{\delta\eta(x'')}\right|_{\eta=\eta_\star[\epsilon]}\\ &= \int dx''\,\frac{\delta^2\eta_\star[\epsilon](x'')}{\delta\epsilon(x)\delta\epsilon(x')}\left.\frac{\delta F_{\rm OP}[\eta]}{\delta\eta(x'')}\right|_{\eta=\eta_\star[\epsilon]} + \int dx''dx'''\,\frac{\delta\eta_\star[\epsilon](x'')}{\delta\epsilon(x)}\frac{\delta\eta_\star[\epsilon](x''')}{\delta\epsilon(x')}\left.\frac{\delta^2 F_{\rm OP}[\eta]}{\delta\eta(x'')\delta\eta(x''')}\right|_{\eta=\eta_\star[\epsilon]}\\ &= \int dx''\,\frac{\delta^2\eta_\star[\epsilon](x'')}{\delta\epsilon(x)\delta\epsilon(x')}\{b\epsilon(x) - g\epsilon(x)^2\eta_\star[\epsilon](x)\} + \{b-2g\epsilon(x)\eta_\star[\epsilon](x)\}\frac{\delta\eta_\star[\epsilon](x)}{\delta\epsilon(x')}\\ &\quad - g\int dx''\,\epsilon(x'')^2\frac{\delta\eta_\star[\epsilon](x'')}{\delta\epsilon(x)}\frac{\delta\eta_\star[\epsilon](x'')}{\delta\epsilon(x')}.\end{aligned} \tag{A14}$$

Summing all three terms, we see a great deal of cancellation, with

$$\frac{\delta^2 F[\eta_\star[\epsilon],\epsilon]}{\delta\epsilon(x)\delta\epsilon(x')} = C_0\delta(x-x') + g\eta_\star[\epsilon](x)^2\delta(x-x') - \{b-2g\epsilon(x)\eta_\star[\epsilon](x)\}\frac{\delta\eta_\star[\epsilon](x)}{\delta\epsilon(x')}.$$

We now need to evaluate this at $\langle\epsilon\rangle$. First, $\eta_\star[\langle\epsilon\rangle] = \langle\eta\rangle$, and

$$\left.\frac{\delta^2 F[\eta_\star[\epsilon],\epsilon]}{\delta\epsilon(x)\delta\epsilon(x')}\right|_{\epsilon=\langle\epsilon\rangle} = C_0\delta(x-x') + g\langle\eta(x)\rangle^2\delta(x-x') - [b-2g\langle\epsilon(x)\rangle\langle\eta(x)\rangle]\left.\frac{\delta\eta_\star[\epsilon](x)}{\delta\epsilon(x')}\right|_{\epsilon=\langle\epsilon\rangle}.$$

Computing the final functional derivative is the most challenging part. We will first compute its functional inverse, take the Fourier transform of that, and then use the basic relationship between Fourier functional inverses to find the form of the noninverse. First, we note

$$\left.\frac{\delta^2 F_{\rm OP}[\eta]}{\delta\eta(x)\delta\eta(x')}\right|_{\eta=\langle\eta\rangle} = \left[r - c_\perp\nabla_\perp^2 - c_\parallel\nabla_\parallel^2 + D\nabla_\perp^4 + 12u\langle\eta(x)\rangle^2\right]\delta(x-x'), \tag{A15}$$

which gives

$$\left(\frac{\delta\eta_\star[\epsilon](x)}{\delta\epsilon(x')}\right)^{\{-1\}}\bigg|_{\epsilon=\langle\epsilon\rangle} = \frac{1}{b-2g\langle\epsilon(x)\rangle\langle\eta(x)\rangle}\left[g\langle\epsilon(x)\rangle^2\delta(x-x') + \frac{\delta^2 F_{\rm OP}[\eta]}{\delta\eta(x)\delta\eta(x')}\right]_{\eta=\langle\eta\rangle}$$
$$= \frac{1}{b-2g\langle\epsilon(x)\rangle\langle\eta(x)\rangle}\left[g\langle\epsilon(x)\rangle^2 + r - c_\perp\nabla_\perp^2 - c_\parallel\nabla_\parallel^2 + D\nabla_\perp^4 + 12u\langle\eta(x)\rangle^2\right]\delta(x-x'). \quad \text{(A16)}$$

Upon substitution of (A3) and expansion to quadratic order $\langle\eta(x)\rangle$, we find

$$\left(\frac{\delta\eta_\star[\epsilon](x)}{\delta\epsilon(x')}\right)^{\{-1\}}\bigg|_{\epsilon=\langle\epsilon\rangle} = \frac{1}{b}\bigg\{r - c_\perp\nabla_\perp^2 - c_\parallel\nabla_\parallel^2 + D\nabla_\perp^4$$
$$+ \langle\eta(x)\rangle^2\left[12u + \frac{b^2 g}{C_0^2} + \frac{2g}{C_0}(r - c_\perp\nabla_\perp^2 - c_\parallel\nabla_\parallel^2 + D\nabla_\perp^4)\right] + O(\langle\eta\rangle^4)\bigg\}\delta(x-x'). \quad \text{(A17)}$$

Defining $\widehat{\langle\eta\rangle^2} = \int dq'\,\langle\hat\eta(q')\rangle\langle\hat\eta(-q')\rangle$, its Fourier transform is then

$$G(q) = \frac{1}{V}\int dx\,dx'\,e^{-iq(x-x')}\left(\frac{\delta\eta_\star[\epsilon](x)}{\delta\epsilon(x')}\right)^{\{-1\}}\bigg|_{\epsilon=\langle\epsilon\rangle}$$
$$= \frac{1}{b}\bigg\{r + c_\perp q_\perp^2 + c_\parallel q_\parallel^2 + Dq_\perp^4 + \widehat{\langle\eta\rangle^2}\left[12u + \frac{b^2 g}{C_0^2} + \frac{2g}{C_0}(r + c_\perp q_\perp^2 + c_\parallel q_\parallel^2 + Dq_\perp^4)\right] + O(\langle\hat\eta\rangle^4)\bigg\}. \quad \text{(A18)}$$

We can now compute $C(q)$ by taking its Fourier transform, using the convolution theorem for the second term:

$$C(q) = C_0 + g\widehat{\langle\eta\rangle^2} - \int dq''\left(b\delta(q'') - \frac{gb}{C_0}\int dq'\langle\hat\eta_{q'}\rangle\langle\hat\eta_{q''-q'}\rangle\right)/G(q-q'')$$
$$= C_0 + g\widehat{\langle\eta\rangle^2} - b^2\left(\frac{1}{r + c_\perp q_\perp^2 + c_\parallel q_\parallel^2 + Dq_\perp^4} - \widehat{\langle\eta\rangle^2}\frac{12u + b^2 g/C_0^2 + \frac{2g}{C_0}(r + c_\perp q^2 + c_\parallel q_\parallel^2 + Dq_\perp^4)}{(r + c_\perp q_\perp^2 + c_\parallel q_\parallel^2 + Dq_\perp^4)^2}\right)$$
$$+ \frac{gb^2}{C_0}\int dq'\,dq''\frac{\langle\hat\eta_{q'}\rangle\langle\hat\eta_{q''-q'}\rangle}{r + c_\perp(q_\perp - q_\perp'')^2 + c_\parallel(q_\parallel - q_\parallel'')^2 + D(q_\perp - q_\perp'')^4} + O(\langle\hat\eta\rangle^4). \quad \text{(A19)}$$

Upon substitution of $\langle\hat\eta_q\rangle = \frac{1}{2}\eta_*[\delta(q_\perp - q_*) + \delta(q_\perp + q_*)]\delta(q_\parallel)$, we have

$$C(q) = C_0 + \frac{1}{4}g\eta_*^2 - b^2\left(\frac{1}{r + c_\perp q_\perp^2 + c_\parallel q_\parallel^2 + Dq_\perp^4} - \frac{\eta_*^2}{4}\frac{12u + b^2 g/C_0^2 + \frac{2g}{C_0}(r + c_\perp q^2 + c_\parallel q_\parallel^2 + Dq_\perp^4)}{(r + c_\perp q_\perp^2 + c_\parallel q_\parallel^2 + Dq_\perp^4)^2}\right)$$
$$+ \frac{gb^2\eta_*^2}{4C_0}\left(\frac{2}{r + c_\parallel q_\parallel^2 + c_\perp q_\perp^2 + Dq_\perp^4} + \frac{1}{r + c_\parallel q_\parallel^2 + c_\perp(q_\perp - 2q_*)^2 + D(q_\perp - 2q_*)^4}\right.$$
$$\left. + \frac{1}{r + c_\parallel q_\parallel^2 + c_\perp(q_\perp + 2q_*)^2 + D(q_\perp + 2q_*)^4}\right) + O(\eta_*^4). \quad \text{(A20)}$$

Evaluating at $q = 0$, we have

$$C(0) = C_0 - \frac{b^2}{r} + \frac{\eta_*^2}{4}\left(g + \frac{b^2}{r^2}(12u + b^2 g/C_0^2) + \frac{2gb^2}{C_0 r}\frac{16Dq_*^4 + 3r}{8Dq_*^4 + r}\right). \quad \text{(A21)}$$

Above the transition this has exactly the form of (18) for any g; below the transition it has the same form at $g = 0$ to order η_*^2. With $r = a\Delta T + c^2/4D + b^2/C_0$, $u = \tilde u - b^2 g/2C_0^2$, and

$$\eta_*^2 = \begin{cases} 0 & \Delta T > 0, \\ -a\Delta T/3\tilde u & \Delta T \leqslant 0, \end{cases} \quad \text{(A22)}$$

we can fit the ratios $b^2/a = 1665\,\text{GPa K}$, $b^2/Dq_*^4 = 6.28\,\text{GPa}$, and $b\sqrt{-g/\tilde u} = 14.58\,\text{GPa}$ with $C_0 = [71.14 - (0.010426\,\text{K}^{-1})T]\,\text{GPa}$. The resulting fit is shown as a dashed black line in Fig. 2.

[1] E. Hassinger, G. Knebel, K. Izawa, P. Lejay, B. Salce, and J. Flouquet, Phys. Rev. B **77**, 115117 (2008).

[2] S. Kambe, Y. Tokunaga, H. Sakai, T. Hattori, N. Higa, T. D. Matsuda, Y. Haga, R. E. Walstedt, and H. Harima, Phys. Rev. B **97**, 235142 (2018).

[3] K. Haule and G. Kotliar, Nat. Phys. **5**, 796 (2009).
[4] H. Kusunose and H. Harima, J. Phys. Soc. Jpn. **80**, 084702 (2011).
[5] H.-H. Kung, R. E. Baumbach, E. D. Bauer, V. K. Thorsmølle, W.-L. Zhang, K. Haule, J. A. Mydosh, and G. Blumberg, Science **347**, 1339 (2015).
[6] F. Cricchio, F. Bultmark, O. Grånäs, and L. Nordström, Phys. Rev. Lett. **103**, 107202 (2009).
Q [7] F. J. Ohkawa and H. Shimizu, J. Phys. **11**, L519 (1999).
[8] P. Santini and G. Amoretti, Phys. Rev. Lett. **73**, 1027 (1994).
[9] A. Kiss and P. Fazekas, Phys. Rev. B **71**, 054415 (2005).
[10] H. Harima, K. Miyake, and J. Flouquet, J. Phys. Soc. Jpn. **79**, 033705 (2010).
[11] P. Thalmeier and T. Takimoto, Phys. Rev. B **83**, 165110 (2011).
[12] S. Tonegawa, K. Hashimoto, K. Ikada, Y. H. Lin, H. Shishido, Y. Haga, T. D. Matsuda, E. Yamamoto, Y. Onuki, H. Ikeda, Y. Matsuda, and T. Shibauchi, Phys. Rev. Lett. **109**, 036401 (2012).
[13] J. G. Rau and H.-Y. Kee, Phys. Rev. B **85**, 245112 (2012).
[14] S. C. Riggs, M. C. Shapiro, A. V. Maharaj, S. Raghu, E. D. Bauer, R. E. Baumbach, P. Giraldo-Gallo, M. Wartenbe, and I. R. Fisher, Nat. Commun. **6**, 6425 (2015).
[15] S. Hoshino, J. Otsuki, and Y. Kuramoto, J. Phys. Soc. Jpn. **82**, 044707 (2013).
[16] H. Ikeda and Y. Ohashi, Phys. Rev. Lett. **81**, 3723 (1998).
[17] P. Chandra, P. Coleman, and R. Flint, Nature (London) **493**, 621 (2013).
7 [18] N. Harrison and M. Jaime, arXiv:1902.06588.
[19] H. Ikeda, M.-T. Suzuki, R. Arita, T. Takimoto, T. Shibauchi, and Y. Matsuda, Nat. Phys. **8**, 528 (2012).
[20] A. de Visser, F. E. Kayzel, A. A. Menovsky, J. J. M. Franse, J. van den Berg, and G. J. Nieuwenhuys, Phys. Rev. B **34**, 8168 (1986).
[21] J. Choi, O. Ivashko, N. Dennler, D. Aoki, K. von Arx, S. Gerber, O. Gutowski, M. H. Fischer, J. Strempfer, M. v. Zimmermann, and J. Chang, Phys. Rev. B **98**, 241113(R) (2018).
[22] S. Ghosh, M. Matty, R. Baumbach, E. D. Bauer, K. A. Modic, A. Shekhter, J. A. Mydosh, E.-A. Kim, and B. J. Ramshaw, Sci. Adv. **6**, eaaz4074 (2020).
[23] P. Chandra, P. Coleman, and R. Flint, J. Phys.: Conf. Ser. **449**, 012026 (2013).
[24] B. Wolf, W. Sixl, R. Graf, D. Finsterbusch, G. Bruls, B. Lüthi, E. A. Knetsch, A. A. Menovsky, and J. A. Mydosh, J. Low Temp. Phys. **94**, 307 (1994).
[25] K. Kuwahara, H. Amitsuka, T. Sakakibara, O. Suzuki, S. Nakamura, T. Goto, M. Mihalik, A. A. Menovsky, A. de Visser, and J. J. M. Franse, J. Phys. Soc. Jpn. **66**, 3251 (1997).
[26] Components of the elastic modulus tensor C were given in the popular Voigt notation in the abstract and Introduction. Here and henceforth, the notation used is that natural for a rank-four tensor.
[27] L. D. Landau, E. M. Lifshitz, A. M. Kosevich, and L. P. Pitaevskii, *Theory of elasticity*, 3rd ed., Landau and Lifshitz
8 Course of Theoretical Physics, Vol. 7 (Pergamon, 1986).
9
[28] B. Lüthi and T. J. Moran, Phys. Rev. B **2**, 1211 (1970).
[29] B. J. Ramshaw, A. Shekhter, R. D. McDonald, J. B. Betts, J. N. Mitchell, P. H. Tobash, C. H. Mielke, E. D. Bauer, and A. Migliori, Proc. Natl. Acad. Sci. U.S.A. **112**, 3285 (2015).
[30] A. Shekhter, B. J. Ramshaw, R. Liang, W. N. Hardy, D. A. Bonn, F. F. Balakirev, R. D. McDonald, J. B. Betts, S. C. Riggs, and A. Migliori, Nature (London) **498**, 75 (2013).
[31] E. M. Lifshitz, Proc. USSR Acad. Sci. J. Phys. **6**, 61 (1942). Q
[32] E. M. Lifshitz, Proc. USSR Acad. Sci. J. Phys. **6**, 251 (1942). Q
[33] P. M. Chaikin and T. C. Lubensky, *Principles of Condensed Matter Physics* (Cambridge University Press, Cambridge, 1995), Chap. 4, Sec. 6.5.
[34] Y. P. Varshni, Phys. Rev. B **2**, 3952 (1970).
[35] C. Bareille, F. L. Boariu, H. Schwab, P. Lejay, F. Reinert, and A. F. Santander-Syro, Nat. Commun. **5**, 4326 (2014).
[36] R. Yoshida, Y. Nakamura, M. Fukui, Y. Haga, E. Yamamoto, Y. Ōnuki, M. Okawa, S. Shin, M. Hirai, Y. Muraoka, and T. Yokoya, Phys. Rev. B **82**, 205108 (2010).
[37] R. Yoshida, K. Tsubota, T. Ishiga, M. Sunagawa, J. Sonoyama, D. Aoki, J. Flouquet, T. Wakita, Y. Muraoka, and T. Yokoya, Sci. Rep. **3**, 2750 (2013).
[38] J.-Q. Meng, P. M. Oppeneer, J. A. Mydosh, P. S. Riseborough, K. Gofryk, J. J. Joyce, E. D. Bauer, Y. Li, and T. Durakiewicz, Phys. Rev. Lett. **111**, 127002 (2013).
[39] C. Broholm, H. Lin, P. T. Matthews, T. E. Mason, W. J. L. Buyers, M. F. Collins, A. A. Menovsky, J. A. Mydosh, and J. K. Kjems, Phys. Rev. B **43**, 12809 (1991).
[40] C. R. Wiebe, J. A. Janik, G. J. MacDougall, G. M. Luke, J. D. Garrett, H. D. Zhou, Y.-J. Jo, L. Balicas, Y. Qiu, J. R. D. Copley, Z. Yamani, and W. J. L. Buyers, Nat. Phys. **3**, 96 (2007).
[41] F. Bourdarot, E. Hassinger, S. Raymond, D. Aoki, V. Taufour, L.-P. Regnault, and J. Flouquet, J. Phys. Soc. Jpn. **79**, 064719 (2010).
[42] E. Hassinger, G. Knebel, T. D. Matsuda, D. Aoki, V. Taufour, and J. Flouquet, Phys. Rev. Lett. **105**, 216409 (2010).
[43] P. Bak, Rep. Prog. Phys. **45**, 587 (1982).
[44] T. Yanagisawa, Philos. Mag. **94**, 3775 (2014).
[45] T. Garel and P. Pfeuty, J. Phys. C **9**, L245 (1976).
[46] T. Inoue, K. Kindo, H. Okuni, K. Sugiyama, Y. Haga, E. Yamamoto, T. C. Kobayashi, Y. Uwatoko, and Y. Onuki, Phys. B (Amsterdam, Neth.) **294–295**, 271 (2001).
[47] G. Ghiringhelli, M. Le Tacon, M. Minola, S. Blanco-Canosa, C. Mazzoli, N. B. Brookes, G. M. De Luca, A. Frano, D. G. Hawthorn, F. He, T. Loew, M. M. Sala, D. C. Peets, M. Salluzzo, E. Schierle, R. Sutarto, G. A. Sawatzky, E. Weschke, B. Keimer, and L. Braicovich, Science **337**, 821 (2012).
[48] R. M. Hornreich, J. Magn. Magn. Mater. **15–18**, 387 (1980).
[49] V. L. Ginzburg, Sov. Phys. Solid State **2**, 1824 (1961). Q
[50] R. Guida and J. Zinn-Justin, J. Phys. A **31**, 8103 (1998).
[51] E. Berg, E. Fradkin, S. A. Kivelson, and J. M. Tranquada, New J. Phys. **11**, 115004 (2009).